Nonlinear frequency conversion in two-dimensional nonlinear photonic crystals solved by a plane-wave-based transfer-matrix method

Jingjuan Li,[1,2] Zhi-Yuan Li,[1,*] and Dao-Zhong Zhang[1]
[1]*Optical Physics Laboratory, Beijing National Laboratory for Condensed Matter Physics, Institute of Physics, Chinese Academy of Sciences, Beijing 100190, People's Republic of China*
[2]*College of Applied Science, Beijing University of Technology, Beijing 100124, People's Republic of China*
(Received 12 June 2007; revised manuscript received 28 September 2007; published 29 May 2008)

We develop the plane-wave-based transfer-matrix method, which is a formalism that has been extensively used to calculate the scattering of electromagnetic waves by usual linear photonic crystals, to solve the quasi-phase-matched (QPM) second-harmonic generation (SHG) in two-dimensional (2D) nonlinear photonic crystals. Using this method, we can calculate the conversion efficiency of high-order collinear and noncollinear QPM second-harmonics. We apply this method to evaluate the SHG conversion efficiency in the 2D periodically poled $LiNbO_3$ crystal with rectangular lattice. The high-order collinear and noncollinear QPM SHGs are observed. The wavelengths at which various orders of QPM SHGs occur and their relative conversion efficiencies predicted by the current theoretical method are in fairly good agreement with those found in experiments. This indicates that the developed method is effective and efficient in handling nonlinear light diffraction in nonlinear photonic crystals.

DOI: 10.1103/PhysRevB.77.195127 PACS number(s): 42.70.Qs, 42.70.Mp, 42.65.Ky, 71.15.Ap

I. INTRODUCTION

Since the experiment on the periodic reversion of the nonlinear susceptibility was demonstrated in 1991,[1] there has been increasing interest in the development of quasi-phase-matched materials. Originally, the conception of quasi-phase-matching (QPM) was restricted to one-dimensional (1D) geometries,[2–6] in which only reciprocal vectors in one direction exist; therefore, the frequency conversion of a single sample is severely limited. In 1998, Berger proposed two-dimensional (2D) nonlinear photonic crystal,[7] which gives out more reciprocal lattices than 1D structure. Afterward, several experimental demonstrations of harmonic generation in 2D nonlinear photonic crystals were successfully presented.[8–10]

However, very few rigorous theoretical approaches have been developed to quantitatively calculate the conversion efficiency in the 2D nonlinear photonic crystals. We have developed transfer-matrix method (TMM) to analyze the problem of second-harmonic generation (SHG) in a 1D multilayer nonlinear optical structure.[11] Wang and Gu[12] solved the wave equation for small-signal sum-frequency process in the 2D nonlinear photonic crystals by the Green's function method. However, the theory employs a free-space Green's function and thus cannot handle a finite length sample with light scattering at its front and back surfaces. In this paper, we will develop the plane-wave-based TMM, which has been used to calculate the photonic band structures for 2D and three-dimensional photonic crystals,[13] to deal with frequency conversion in quasi-phase-matched materials. We will investigate in detail the plane-wave-based TMM that can efficiently deal with SHG problem in 2D nonlinear quasi-phase-matched materials and apply this approach to calculate the conversion efficiency for 2D periodical nonlinear photonic crystals with rectangular lattice. Comparison will be made between the theoretical results calculated by this method and experimental results.

II. PLANE-WAVE-BASED TMM FOR SECOND-HARMONIC GENERATION IN TWO-DIMENSIONAL PERIODICAL NONLINEAR PHOTONIC CRYSTALS

We now consider a 2D nonlinear photonic crystal. The nonlinear susceptibility $\chi^{(2)}$ of the sample is periodically modulated on the yz plane, and the polarization direction of the domains is along the x axis or inverse. The nonlinear sample is a finite-thickness slab along the z-axis direction. The extension in the lateral direction (y axis) is much larger and is assumed to be infinite in our simulation. Here, we only consider orthogonal-lattice structures. The formalism can be readily extended to other lattice structures. Figure 1 illustrates a microscopic picture of the 2D poled nonlinear photonic crystal with rectangular lattice. The circular areas in the picture are reversed domains, in which the polarization direction of the domains is along the anti-x-axis, while in the background area, the polarization direction of the domains is along the x axis. The primitive lattice of the nonlinear photonic crystal has two unit vectors a_1 and a_2 along the z axis and y axis, respectively. The corresponding reciprocal lattice $\boldsymbol{G}$ has two unit vectors of b_1 and b_2. It is assumed that a plane-wave laser beam is launched upon the sample from its left side along the z-axis direction. We will consider a general situation beyond the usual normal-incidence condition. The inclined incident angle is denoted by θ with respect to

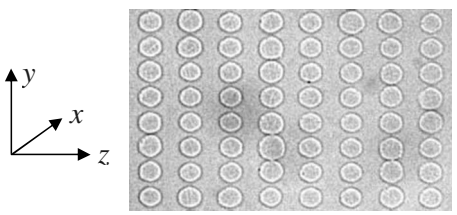

FIG. 1. Optical micrograph of the etched 2D poled nonlinear photonic crystal with rectangular lattice. The periods of the rectangular lattice are, respectively, 13.64 and 8.48 μm.

the z axis; thus, the incident wave vector is $k_{10}=(k_{10,y},k_{10,z})$. When $\theta=0^0$, we return to the usual experimental situation of normal incidence. The polarization of the incident electric field is along the x axis. In the following, we solve the conversion efficiency of this structure by the transfer-matrix method.

In a nondepleted pump wave approximation, the electric field of fundamental field (FW) in the medium can be expressed as

$$E_1(y,z) = E_1(z)\exp(ik_{1,y}y) = \{\Omega^+ \exp[ik_{1,z}(z-z_0)] + \Omega^- \exp[-ik_{1,z}(z-z_0)]\}\exp(ik_{1,y}y), \quad (1)$$

where $k_{1,y}^2+k_{1,z}^2=k_1^2$, $k_1=n_1k_{10}$, and $k_{10}=\omega/c$. ω is the frequency of FW. n_1 is the refractive index of the material at the FW frequency and c is the group velocity of light in vacuum. z_0 is the boundary of the sample and we set $z_0=0$. Ω^+ (Ω^-) represent the amplitude of the forward (backward) FW within the nonlinear crystal slab.

Using the transfer-matrix method, which is described in detail in Ref. 11, we can get the following relationship between the amplitudes of the electric field of FW on the right and left sides of the structure,

$$\begin{pmatrix} \Omega_t^+ \\ \Omega_t^- \end{pmatrix} = D_0^{-1}D_1P_1D_1^{-1}D_0\begin{pmatrix} \Omega_0^+ \\ \Omega_0^- \end{pmatrix}, \quad (2)$$

where $\Omega_0^{\pm}$ and $\Omega_t^{\pm}$ denote the amplitudes of the electric field of FW on the left and right sides of the structure, respectively. The matrices in Eq. (2) are defined as

$$D_0 = \begin{pmatrix} 1 & 1 \\ \frac{k_{10,z}}{k_{10}} & -\frac{k_{10,z}}{k_{10}} \end{pmatrix}, \quad D_1 = \begin{pmatrix} 1 & 1 \\ \frac{k_{1,z}}{k_{10}} & -\frac{k_{1,z}}{k_{10}} \end{pmatrix},$$

$$P_1 = \begin{pmatrix} \exp(ik_{1,z}d) & 0 \\ 0 & \exp(-ik_{1,z}d) \end{pmatrix},$$

where d is the thickness of the structure.

From Eq. (2), we can solve the relative amplitudes $\Omega^{\pm}$ for FW within the nonlinear crystal slab. Then, the fundamental wave inside medium at arbitrary position can be determined as

$$E_1(y,z) = E_1(z)\exp(ik_{1,y}y), \quad (3)$$

with

$$E_1(z) = [\Omega^+ \exp(ik_{1,z}z) + \Omega^- \exp(-ik_{1,z}z)]. \quad (4)$$

We now turn to consider the second harmonic wave (SHW). In the case of two dimensions, the propagation equation for the electric field of SHW is

$$(\partial^2/\partial z^2 + \partial^2/\partial y^2)E_2(y,z) + k_2^2E_2(y,z) = -k_{20}^2\chi^{(2)}(r)[E_1(y,z)]^2, \quad (5)$$

where $k_2=n_2k_{20}$ and $k_{20}=2\omega/c$. n_2 is the refractive index of the material at the SHW frequency and $\chi^{(2)}(r)$ is the periodical nonlinear susceptibility of the nonlinear photonic crystal. Here, the SI units are adopted.

In the case of two dimensions, the nonlinear susceptibility periodically varies in the 2D plane. In order to solve the unknown electromagnetic fields of SHW, we divide each period of the nonlinear photonic crystal into a number of thin slices (M slices in total, for example) along the wave propagation direction (namely, the z axis), as shown in Fig. 2(a). Each slice can be approximated as a lamellar 1D grating, within which the nonlinear susceptibility is constant along the z-axis direction. We further imagine that each slice is surrounded by an infinitely thin film of air in both hand sides. With a zero thickness, these artificial air thin films will generate no impact. Inclusion of these auxiliary air films will bring much convenience to solve the SHG problem by the transfer-matrix method since the background material for the nonlinear crystal slab is air. In addition, the geometric configuration will allow us to handle more complicated structure where both the linear $n(r)$ and the nonlinear susceptibilities $\chi^{(2)}(r)$ are periodically modulated in a very convenient way.[13,14]

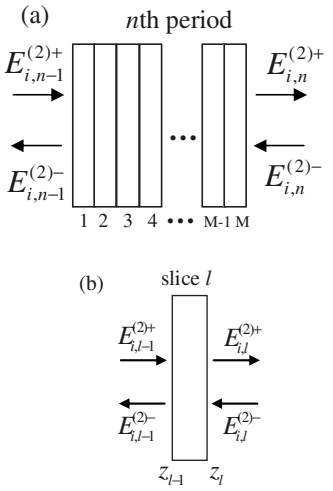

FIG. 2. (a) One period of nonlinear photonic crystal, which is divided into a number of thin films along the propagation direction. (b) An individual slice, around which the electromagnetic field consists of forward and backward propagating waves.

For the lth slice, we can write down the plane-wave expansion expression of the nonlinear susceptibility,

$$\chi_l^{(2)}(r) = \sum_j \chi_{j,l}\exp(iG_{j,y}y), \quad (6)$$

where $G_{j,y}=jb_2$ and $\chi_{j,l}$ is the expansion coefficients, which can be calculated by the inverse Fourier Transform. The electric field of SHW at an arbitrary point $\mathbf{r}$ can also be written into the superposition of Bragg waves (or plane waves),

$$E_2(y,z) = \sum_j E_j(z)\exp(ik_{2j,y}y), \quad (7)$$

where the Bragg wave vector $k_{2j,y}=k_{2,y}+jb_2=2k_{1,y}+G_{j,y}$, which is the QPM condition for the transverse wave vector. $E_j(z)$ is the unknown expansion coefficient of the electric field and b_2 is the unit vector of reciprocal lattice along the y axis. In principle, the indices j should run from $-\infty$ to $+\infty$, but in numerical practice, truncation over a certain order is necessary.

Substituting Eqs. (6) and (7) into Eq. (5) yields the propagation equation for the electric field of SHW in the lth slice as

$$\partial^2 E_{j,l}(z)/\partial z^2 + k_{2j,z}^2 E_{j,l}(z) = -k_{20}^2 \chi_{j,l}[E_{1,l}(z)]^2, \tag{8}$$

where $E_{j,l}(z)$ is the electric field of SHW, which is equivalent to $E_j(z)$ in Eq. (7) and the subscript l denotes the lth slice. $k_{2j,z}$ is given by $k_{2j,z}=(k_2^2-k_{2j,y}^2)^{1/2}$ for $k_2^2-k_{2j,y}^2 \geq 0$ and $k_{2j,z}=i(k_{2j,y}^2-k_2^2)^{1/2}$ for $k_2^2-k_{2j,y}^2<0$. Substituting Eq. (4) into Eq. (8), we can get an equation just like Eq. (9) in Ref. 11, and so we can get the expression of electromagnetic field in 2D structure through the same step to achieve Eq. (12) in Ref. 11,

$$\begin{pmatrix} E_{j,l}(z) \\ H_{j,l}(z) \end{pmatrix} = G_j \begin{pmatrix} U_{j,l}^+(z) \\ U_{j,l}^-(z) \end{pmatrix} + BA(j,l) \begin{pmatrix} (\Omega^+)^2(z) \\ (\Omega^-)^2(z) \end{pmatrix} + \begin{pmatrix} 1 \\ 0 \end{pmatrix} C(j,l) 2\Omega^+\Omega^-, \tag{9}$$

with the expressions

$$U_{j,l}^{\pm}(z) = U_{j0}^{\pm} \exp[\pm ik_{2j,z}(z-z_{l-1})],$$
$$(\Omega^{\pm})^2(z) = (\Omega^{\pm})^2 \exp(\pm i2k_{1,z}z),$$
$$G_j = \begin{pmatrix} 1 & 1 \\ \frac{k_{2j,z}}{k_{20}} & -\frac{k_{2j,z}}{k_{20}} \end{pmatrix}, \quad B = \begin{pmatrix} 1 & 1 \\ \frac{2k_{1,z}}{k_{20}} & -\frac{2k_{1,z}}{k_{20}} \end{pmatrix},$$
$$A(j,l) = \frac{-k_{20}^2 \chi_{j,l}}{k_{2j,z}^2 - 4k_{1,z}^2}, \quad C(j,l) = \frac{-k_{20}^2 \chi_{j,l}}{k_{2j,z}^2},$$

where U_{j0}^+ and U_{j0}^- represent the unknown amplitudes of the forward and backward SHWs at the boundary.

Having written down the electromagnetic fields inside the grating slice, we need to further solve the electromagnetic fields in the air thin films around the slice. As shown in Fig. 2(b), the electric field of SHW in the two air thin films around the lth slice is both consisting of forward- and backward-propagating plane waves. The electric field on the right-hand-side air film can be written into

$$E_l^{(2)}(z) = \sum_j [E_{j,l}^+(z) + E_{j,l}^-(z)] \exp(ik_{20,y}y), \tag{10}$$

where $E_{j,l}^{\pm}(z)=E_{j,l}^{(2)\pm} \exp[\pm ik_{20,z}(z-z_l)]=E_{j,l}^{(2)\pm}$ since $z=z_l$.

The electric and magnetic fields of SHW in the air films can also be written into a concise form, just as Eq. (9),

$$\begin{pmatrix} E_{j,l}(z) \\ H_{j,l}(z) \end{pmatrix} = \begin{pmatrix} 1 & 1 \\ \frac{k_{20,z}}{k_{20}} & -\frac{k_{20,z}}{k_{20}} \end{pmatrix} \begin{pmatrix} E_{j,l}^{(2)+} \\ E_{j,l}^{(2)-} \end{pmatrix} = G_0 \begin{pmatrix} E_{j,l}^{(2)+} \\ E_{j,l}^{(2)-} \end{pmatrix}. \tag{11}$$

The electromagnetic fields on the left-hand-side air film have the same form.

Considering the continuous condition of the electric and magnetic fields at the interfaces of the lth slice $z=z_l$ and $z=z_{l-1}$, we can get the relation of the second-harmonic (SH) field through the lth slice,

$$\begin{pmatrix} E_{j,l}^{(2)+} \\ E_{j,l}^{(2)-} \end{pmatrix} = G_0^{-1} T G_0 \begin{pmatrix} E_{j,l-1}^{(2)+} \\ E_{j,l-1}^{(2)-} \end{pmatrix} + G_0^{-1}(BF-TB)A(j,l) \times \begin{pmatrix} (\Omega^+)^2(z_{l-1}) \\ (\Omega^-)^2(z_{l-1}) \end{pmatrix} + G_0^{-1}(1-T) \begin{pmatrix} 1 \\ 0 \end{pmatrix} C(j,l) 2\Omega^+\Omega^-, \tag{12}$$

where

$$T = G_j Q_j G_j^{-1}, \quad Q_j = \begin{pmatrix} \exp(ik_{2j,z}h_l) & 0 \\ 0 & \exp(-ik_{2j,z}h_l) \end{pmatrix},$$
$$F = \begin{pmatrix} \exp(i2k_{1,z}h_l) & 0 \\ 0 & \exp(-i2k_{1,z}h_l) \end{pmatrix},$$

$h_l=z_l-z_{l-1}$ is the thickness of the lth slice.

Considering M slices in one period of the nonlinear structure, we can cascade Eq. (12) M times and get the overall transfer matrix of the SH signal for one period of nonlinear structure as

$$\begin{pmatrix} E_{j,n}^{(2)+} \\ E_{j,n}^{(2)-} \end{pmatrix} = S \begin{pmatrix} E_{j,n-1}^{(2)+} \\ E_{j,n-1}^{(2)-} \end{pmatrix} + \begin{pmatrix} E_{j,n}^t \\ E_{j,n}^r \end{pmatrix}, \tag{13}$$

where

$$\begin{pmatrix} E_{j,n}^t \\ E_{j,n}^r \end{pmatrix} = \sum_{l=1}^{M} G_0^{-1} T^{M-l} \left[(BF-TB)A(j,l) \begin{pmatrix} (\Omega_{n,l}^+)^2 \\ (\Omega_{n,l}^-)^2 \end{pmatrix} + (1-T) \times \begin{pmatrix} 1 \\ 0 \end{pmatrix} C(j,l) 2\Omega^+\Omega^- \right],$$

$(\Omega_{n,l}^{\pm})^2=(\Omega^{\pm})^2 \exp\{\pm i2k_{1,z}[(n-1)a_1+(l-1)h_l-z_0]\}$ and $S=G_0^{-1}T^M G_0$. n denotes the nth period and l denotes the number of slice in one period.

As a recursive equation, Eq. (13) serves as the unit transfer matrix of the SH field for the nth period. From this equation, we can get the overall transfer matrix of the SH signal for the whole nonlinear structure. Considering the periodicity of the structure, we get the forward and backward radiations of the SH fields radiated from a nonlinear structure composed of N periods along the propagation direction by the following recursion formalism:

$$\begin{pmatrix} E_{t,j}^{(2)+} \\ 0 \end{pmatrix} = S^N \begin{pmatrix} 0 \\ E_{0,j}^{(2)-} \end{pmatrix} + \sum_{n=1}^{N} S^{N-n} \begin{pmatrix} E_{j,n}^t \\ E_{j,n}^r \end{pmatrix}. \tag{14}$$

From Eq. (14), we can calculate $E_{t,j}^{(2)+}$ and $E_{0,j}^{(2)-}$ and the conversion efficiencies of the forward and backward waves are evaluated, respectively, by

$$\eta_{\text{forth}} = \frac{\sum_j |E_{t,j}^{(2)+}|^2}{|\Omega_0^+|^2} \quad \text{and} \quad \eta_{\text{back}} = \frac{\sum_j |E_{0,j}^{(2)-}|^2}{|\Omega_0^+|^2}.$$

III. FREQUENCY CONVERSION IN 2D RECTANGULAR LATTICES

We now investigate a simple 2D nonlinear photonic crystal with rectangular lattice of poled circular cylinders, which

has been studied by experiment.[15,16] Figure 1 is the microscopic picture of the etched sample. The lattice constants of the nonlinear photonic crystal are 13.64 and 8.48 μm, the same as the values in Ref. 15. The corresponding reciprocal lattice vectors are, respectively, 0.461 and 0.741 μm^{-1}. The radius of poled circular cylinder is set to 3.51 μm. The sample is chosen as $LiNbO_3$ crystal. Its nonlinear coefficient d_{33} is 47.0 pm/V,[17] and its refractive index for extraordinary light is given by the following dispersion formula:[18]

$$n_e^2 = a_1 + b_1 f + \frac{a_2 + b_2 f}{\lambda^2 - (a_3 + b_3 f)^2} - a_4 \lambda^2,$$

where $a_1=4.5820$, $a_2=0.099\ 21$, $a_3=0.210\ 90$, $a_4=0.021\ 940$, $b_1=2.2971\times10^{-7}$, $b_2=5.2716\times10^{-8}$, $b_3=-4.191\ 43\times10^{-8}$, $f=(T-T)_0(T+T_0+546)$, and $T_0=24.5\ ^\circ$C. At room temperature, the value of variable f is set to zero. λ is the wavelength in the vacuum and the unit is micrometer.

The effective QPM SHG in a 2D nonlinear crystal must satisfy the momentum conservation $k_{2\omega}-2k_{\omega}-G_{m,n}=0$, where $G_{m,n}$ is the reciprocal lattice vector of the nonlinear photonic crystals and (m,n) is the order of QPM. The (m,n)-order QPM in 2D periodic structure means that the total m basic vectors along one basic direction and n basic vectors along another direction are adopted. As an example, $G_{0,1}$ or $G_{1,0}$ and $G_{0,2}$ or $G_{2,0}$ are, respectively, called first- and second-order QPMs, in which the fundamental and second-harmonic wave vectors are collinear. In the case of

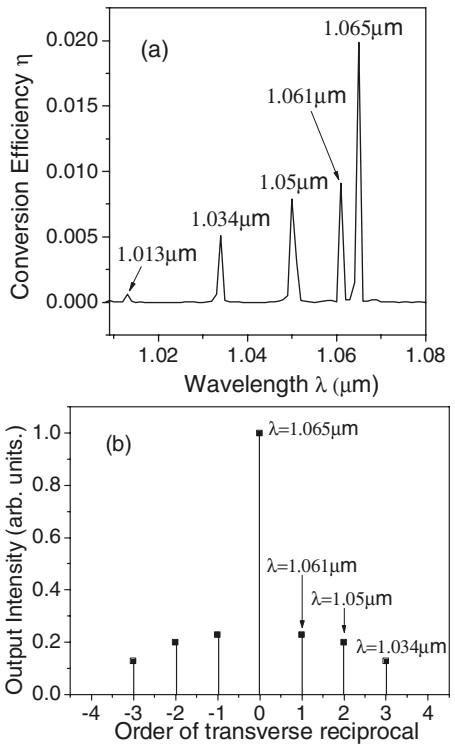

FIG. 3. (a) Calculated conversion efficiency of $(\pm m,2)$-order QPM second-harmonic wave as a function of the incident fundamental wavelength. (b) The relative intensities of SH outputs against the order of transverse reciprocal lattice vector m.

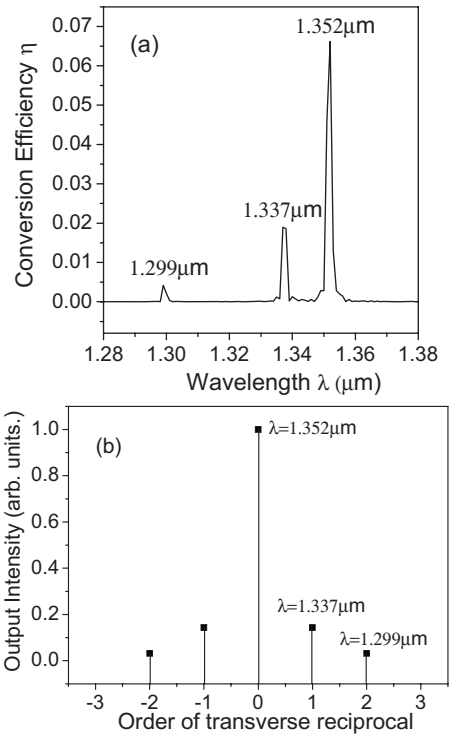

FIG. 4. (a) Calculated conversion efficiency of $(\pm m,1)$-order QPM second-harmonic wave as a function of the incident fundamental wavelength. (b) The relative intensities of SH outputs against the order of transverse reciprocal lattice vector m.

$m\neq0$ and $n\neq0$, the corresponding QPM becomes noncollinear.

We first study the $(\pm m,2)$-order $(m=0,1,2,3,\ldots)$ QPM along the longer period direction in the rectangular lattice, which has been experimentally studied in Ref. 15. The sample we studied contains 300 periods (about 4 mm) along the propagation direction. The pump light is a continuous wave and is normally incident upon the nonlinear crystal slab sample. As a comparison, in experiment,[15] the sample is 8 mm long and the pump light is pulse. In our numerical calculation, we have tuned the wavelength of the incident fundamental wave and solve the conversion efficiencies for different incident waves. The results are shown in Fig. 3(a). When we tune the wavelength of the incident wave, the incidental direction is unchanged. There are several peaks of SH outputs in Fig. 3(a). The corresponding wavelengths of peaks are 1.065,1.061, 1.05, 1.034, and 1.013 μm, which is basically in agreement with the results in Ref. 15. The SH output in the experiment correspond to the input wavelengths of 1.069, 1.062, 1.052, 1.037, and 1.013 μm. The slight differences between our results and experimental results in regard to the SHG wavelength is attributed to the short range structural disorder unintentionally introduced during the fabrication process in the experiment. When the intensity of the incident fundamental wave sets $I=84.94$ GW/m^2, corresponding to $|E_1|^2=64$ V$^2/\mu$m^2, the conversion efficiencies of these SHs are about 1.99, 0.91, 0.79, 0.51, and 0.06%, respectively. These numbers of conversion efficiencies are lower than those in Ref. 15. However, the original conditions we used are power of the pump light and square of the length

of the sample. So, by using high power input and increasing the length of the sample, we can get higher conversion efficiencies.

The phase matching of these SH outputs with different wavelengths must be realized by different reciprocal lattice vectors. There are not only the collinear SHGs but also the noncollinear ones, in which the high-order transverse reciprocal lattice vectors must be used. Using the method we developed, we can find which transverse reciprocal lattice vectors are used for a certain input fundamental wave. Figure 3(b) illustrates the relative intensities of those peaks in Fig. 3(a) and the abscissa denotes the order of transverse reciprocal lattice vectors. From Fig. 3(b), we can clearly see that the reciprocal lattice vectors, corresponding to the QPM SH outputs of 1.065, 1.061, 1.05, and 1.034 μm, are $G_{0,2}$, $G_{\pm 1,2}$, $G_{\pm 2,2}$, and $G_{\pm 3,2}$, respectively. Combining Figs. 3(a) and 3(b), we can find that the less the value of (m,n), the larger the conversion efficiency of SH, which is also consistent with the conclusion in Ref. 15.

We also present the results of $(\pm m,1)$-order QPM in Fig. 4. Figure 4(a) is the conversion efficiency as a function of wavelengths of incident FW. Figure 4(b) illustrates the relative intensities of different incident waves and the abscissa gives the order of transverse reciprocal lattice vectors used in the process of QPM SHG. Figure 4 indicates that we can achieve the QPM SHG for the wavelengths of 1.352, 1.337, and 1.299 μm, and the corresponding reciprocal lattice vectors are $G_{0,1}$, $G_{\pm 1,1}$ and $G_{\pm 2,1}$. Considering the disorder of structure unintentionally introduced in the experiment, our results and experimental results are in fairly good agreement. When the intensity of the incident fundamental wave is set to be $I=11.94$ GW/m^2, corresponding to $|E_1|^2=9$ V$^2/\mu$m^2, the conversion efficiencies of these SHs are about 6.62, 1.9, and 0.42%, respectively. The conversion efficiencies can also be enhanced by increasing the length of the sample and the power of input fundamental wave. High-order QPM third harmonics are not present in our results, which was generated in the experiment, because we do not consider the cascading processes in our theoretical method.

IV. CONCLUSIONS

In summary, we have extended the plane-wave-based TMM from its routine service as a powerful tool to solve electromagnetic wave scattering by a general multilayer grating and photonic crystal slab to handle the QPM SHG in the 2D nonlinear photonic crystals. Using this method, we can calculate the conversion efficiency of SH and find out which transverse reciprocal lattice vector is used to realize the QPM for a certain input fundamental wave. We have applied this method to evaluate the QPM SHG conversion efficiency in the 2D periodically poled $LiNbO_3$ crystal with rectangular lattice. The high-order collinear and noncollinear QPM SHGs have been observed. The theoretical results calculated with the current method agreed well with the experimental results in regard to the wavelengths at which various orders of QPM SHG occur and their relative conversion efficiencies. This indicates that the developed method is effective and efficient in handling nonlinear light diffraction in nonlinear photonic crystals.

ACKNOWLEDGMENTS

This work was supported by the National Natural Science Foundation of China under Grants No. 10525419 and No. 10474135 and by the National Key Basic Research Special Foundation of China under Grant No. 2006CB921702.

*Corresponding author; lizy@aphy.iphy.ac.cn

[1] S. Matsumoto, E. J. Lim, H. M. Hertz, and M. M. Fejer, Electron. Lett. **27**, 2040 (1991).
[2] J. H. Kim and C. S. Yoon, Appl. Phys. Lett. **81**, 3332 (2002).
[3] K. R. Parameswaran, J. R. Kurz, R. V. Roussev, and M. M. Fejer, Opt. Lett. **27**, 43 (2002).
[4] S. N. Zhu, Y. Y. Zhu, Z. J. Yang, H. F. Wang, Z. Y. Zhang, and N. B. Ming, Appl. Phys. Lett. **67**, 320 (1995).
[5] D. Taverner, P. Britton, P. G. R. Smith, D. J. Richardson, G. W. Ross, and D. C. Hanna, Opt. Lett. **23**, 162 (1998).
[6] L. M. Zhao and B. Y. Gu, Appl. Phys. Lett. **88**, 161909 (2006).
[7] V. Berger, Phys. Rev. Lett. **81**, 4136 (1998).
[8] N. G. R. Broderick, G. W. Ross, H. L. Offerhaus, D. J. Richardson, and D. C. Hanna, Phys. Rev. Lett. **84**, 4345 (2000).
[9] A. Chowdhury, C. Staus, B. F. Boland, T. F. Kuech, and L. McCaughan, Opt. Lett. **26**, 1353 (2001).
[10] P. G. Ni, B. Q. Ma, Y. H. Liu, B. Y. Cheng, and D. Z. Zhang, Jpn. J. Appl. Phys., Part 1 **44**, 1269 (2005).
[11] J. J. Li, Z. Y. Li, and D. Z. Zhang, Phys. Rev. E **75**, 056606 (2007).
[12] X. H. Wang and B. Y. Gu, Eur. Phys. J. B **24**, 323 (2001).
[13] Z. Y. Li and L. L. Lin, Phys. Rev. E **67**, 046607 (2003).
[14] P. M. Bell, J. B. Pendry, L. Marin Moreno, and A. J. Ward, Comput. Phys. Commun. **85**, 306 (1995).
[15] B. Q. Ma, T. Wang, P. G. Ni, B. Y. Cheng, and D. Z. Zhang, Europhys. Lett. **68**, 804 (2004).
[16] P. G. Ni, B. Q. Ma, S. Feng, B. Y. Cheng, and D. Z. Zhang, Opt. Commun. **233**, 199 (2004).
[17] V. G. Dmitriev, G. G. Gurazdyan, and D. N. Nikogosyan, *Handbook of Nonlinear Optical Crystals* (Springer, Berlin, 1997).
[18] G. J. Edwards and M. Lawrence, Opt. Quantum Electron. **16**, 373 (1984).